Int. J. Nano Dimens., 13 (1): 105-116, Winter 2022

ORIGINAL ARTICLE

Synthesis and characterization of Tetrachloromenthoxyphosphor@ TiO_2 nanocomposite as a high-performance photocatalyst for catalytic degradation of methyl violet

Mohammad Saim Rahmatyan[1], Zahra Shokri Aghbolagh[1], Shahriar Ghammamy[1], Nafise Gharagozloo[1], Maryam Mahdavinia[1], Soheil Zabihi[2]*

[1] *Department of Chemistry, Faculty of Science, Imam Khomeini International University, Qazvin, Iran*
[2] *Department of Chemistry, Faculty of Science, Islamic Azad University, Ardabil Branch, Ardabil, Iran*

Received 01 June 2021; revised 12 September 2021; accepted 17 September 2021; available online 22 September 2021

Abstract

In this research, a new organic–inorganic hybrid photocatalyst (TCMP@TiO_2) was successfully synthesized through supporting tetrachloromenthoxyphosphor (III) (TCMP) on titanium dioxide (TiO_2) for elimination of methyl violet (MV) color from water media. The hybrid inorganic-organic catalyst of this nanocomposite was characterized by 1H-NMR, 31P-NMR, 13C-NMR, UV-Vis, IR, SEM, and mass spectrometry methods. The maximum dye elimination and significance of variables on the dye removal system in static condition were evaluated by response surface methodology (RSM). The maximum dye removal (83.6%) of MV was obtained under optimum conditions (0.02 g catalyst dosage, 35 °C, and pH 8) in the presence of 1.5 mM of hydrogen peroxide. The higher regression coefficient of the response and the variables (R^2=0.9275) showed a well investigation of the outcomes by a regression-based polynomial model. In comparison with the previously reported photocatalytic decolorization systems, the dye removal system suggested in this work is quick, easy, and involves a small amount of catalyst. This new photocatalyst shows potent visible-light photocatalytic activity for the decolorization of methyl violet, due to the generation the strong oxidants hydroxyl radical (OH) and superoxide anion radical ($O_{2.}$) via photoelectrochemical decomposition of H_2O and O_2 in the presence of visible light irradiation. These outcomes proposed that TCMP@TiO_2 could be applied for significant removal of dyes from textile wastewater.

Keywords: *Characterization; Decolorization; Experimental Design; Hybrid Photocatalyst; Nanocomposite; Substituted Organophosphorus.*

How to cite this article

Saim Rahmatyan M., Shokri Aghbolagh Z., Ghammamy Sh., Gharagozloo N., Mahdavinia M., Zabihi S. Synthesis and characterization of Tetrachloromenthoxyphosphor@TiO_2 nanocomposite as a high-performance photocatalyst for catalytic degradation of methyl violet. Int. J. Nano Dimens., 2022; 13(1): 105-116.

INTRODUCTION

Synthetic colors are considerably applied for textile coloring operations, with around 50% of such chemical structures being azo-based dyes [1-2]. Such materials are analyzed based on their azo groups (–N=N–), that are the dye type, and the existence of $–NH_2$, –OH, $–CH_3$, and $–SO_3$ functional groups are important for the fascination of these dye materials to fibers [3]. Almost all azo-based dyes are treated to be actually stable utilizing general methods such as active sludge or oxidative techniques, as well as physicochemical treatment [3-9]. Thus, improvement of new and promising technologies against harmful effluents is a need of the current era, since of the quantity of effluents is expanding exponentially. In the present research, methyl violet (MV, $C_{24}H_{28}N_3Cl$) was applied as the pollution agent. Methyl violet is a traditional industrial dye recommended for its stability and is grouped as an azo-dye. Azo-compounds, which are manufactured inorganic chemical structures, claim up to 70% of the dyes in use in present era

* Corresponding Author Email: *shghamami@ikiu.ac.ir*
shghamami@yahoo.com

[10]. The deliverance of this effluent is considered "non- aesthetic pollutant" since amounts less than 1 ppm can be seen in water media. However, this is the constitutional motivation for degrading methyl violet; the color wastewater can also produce toxic by-products during different reactions such as oxidation and hydrolysis [10]. As mentioned, these azo-chemical compounds are very stable, which is because of the large proportion of aromatics in the color. Based on the hard-degrading pollutions such as MV, a process recommended to as oxidation mechanism was proposed as another option for water purification. It has been investigated that heterogeneous photocatalysts, such as TiO_2, are the most damaging with regard to azo-compounds [10]. TiO_2 are commonly used for photocatalytic decolorization in commercial utilization, but a separation procedure is required to recover back the TiO_2 powder from the considered effluent, which enhances the whole capital and running cost [11]. This has led to studies on immobilizing TiO_2 on various supporting compounds that can fulfill some essentials; reusability with retained TiO_2 photoactivity, ease of preparation, and being eco-friendly. Newly, elemental semiconductors, such as phosphorus-based compounds, have received much attention as a photocatalysis. It is maybe due to their unique properties, such as high absorption of visible light, low cost, and earth abundance [12-13]. As such, tetrachloromenthoxyphosphor (III) could be applied as a proper solid support to paralyze the catalyst [14-15]. This material from the organophosphorus family can be proper ligands for transitional metals (especially lanthanides) which, together with the interesting structural properties advised by chemists, can be in the form of molecules that indicate action like zeolites. Further, these molecules can be applied as a suitable adsorbent for specific transitional metal cations from wastewater plants act [16]. The utilization of organophosphorus molecules along with titanium dioxide, which with its hydrophilic and photocatalytic properties, has an important role in eliminating dyes and pollutants from industrial wastewater, rising the influence of dye removal of textile wastewaters. We had previously described preliminary findings on the capacity of TCMP@TiO_2 composite to properly decolorize standard dyes such as methylene violet [17]. In this research, we optimized the system variables for the dye removal process. The suitability of the cast TCMP@TiO_2 in evaluating real industrial batik dye effluent was also explained and expressed in terms of dye removal. The outcomes of this work aim to help in the extension of a simple, effective, inexpensive, and reusable approach for analysis of textile effluents.

EXPERIMENTAL

Materials and Instruments

All materials applied in this work were purchased from Merck Company. Titanium dioxide powder (TiO_2) (Degussa P-25, ca. 80% anatase, 20% rutile) were utilized as starting component with a BET surface area of 50 m^2/g. The deionized water (DIW) was used in all processes of the experiments. Mass spectra were achieved on an Agilent Technology (HP) model Network Mass Selective Detector 5973 spectrophotometer. XRD patterns were obtained on a D8 Bruker Advanced X-ray diffractometer applying Cu kα radiation (α=1.54 ˚A). The patterns were processed within the 2θ range with a continuous scan mode. The FT-IR spectra were obtained by a Matson FT-IR spectrophotometer using KBr disks within the region of 400–4000 cm^{-1}. The UV−Vis spectra of the solutions were processed utilizing the Shimadzu UV-160 spectrophotometer. Following the dye degradation process, the samples were studed by UV–Vis spectroscopy (a double beam Thermo-Heylos spectrometer), applying quartz cells with a path length of 10-mm. ^{31}P nuclear magnetic resonance (^{31}P– NMR) data were obtained applying Bruker Ultra Shield 250 MHz.

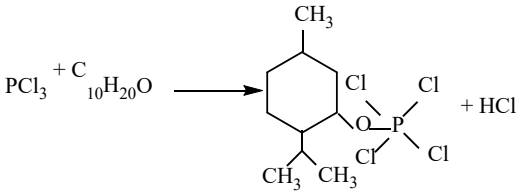

Synthesis of tetrachloromenthoxyphosphor (III) (TCMP)

Tetrachloromenthoxyphosphor was processed by dissolving powdered 2-Isopropyl-5-methylcyclohexanol (menthol) in PCl_5 and stirred for 1h at room temperature, keeping the ratio of $C_{10}H_{19}OH$: PCl_5 as 1:1. The stirring continued until the product was prepared, then the system was filtered where clear solution without any color was laid-off along with the excitement was a sign that this is an output of the reaction. Anal.

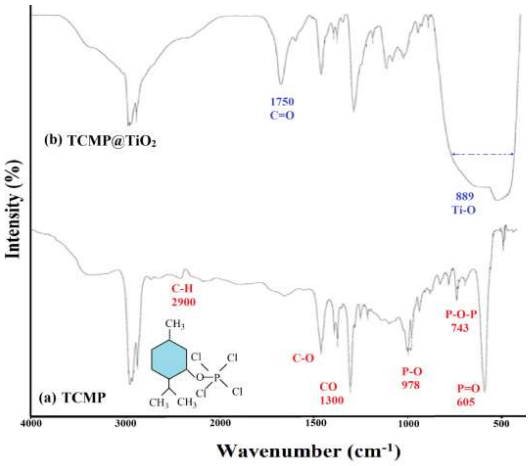

Fig. 1. FT-IR of (a) TCMP, (b) TCMP@TiO_2.

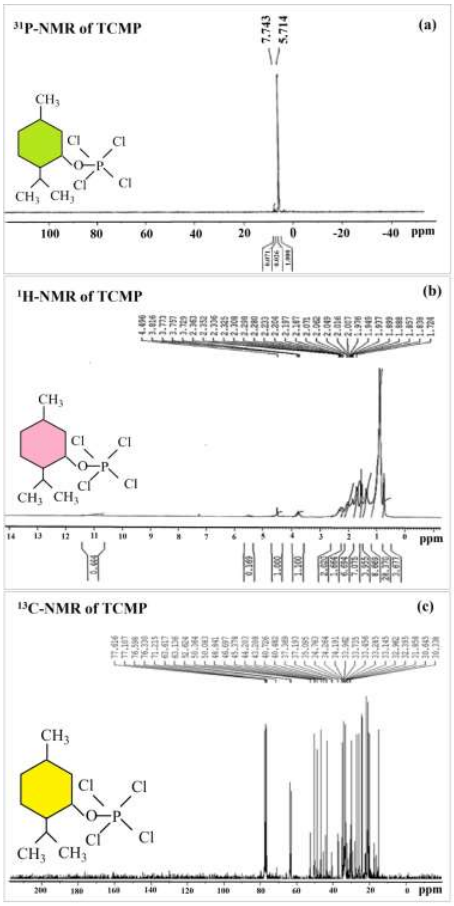

Fig. 2. (a) The 31P-NMR, (b) 1H-NMR, and (c) 13C-NMR of TCMP structure.

Calc. for $C_{10}H_{19}PClO$: C, 36.63; H, 5.79. Figure out: C, 36.90; H, 5.81. IR (KBr) (cm^{-1}): 3359, 2955, 1456, 1369, 1302, 734, 775, 589, 484, cm^{-1} (Fig.1 (a)). ^{31}P-NMR (135 MHz, $CDCl_3$): δ= 5.714 ppm (Fig. 2 (a)). ^{1}H-NMR (250 MHz, $CDCl_3$) δ= 3.7(s), 1.9(d), 1.6(d), 1.3(t), 1.35(t), 0.9(d) (Fig. 2 (b)). ^{13}C-NMR (250 MHz, CD_3CN): δ= 30.33, 31.85, 24.3, 33.45, 35.09, 50.36, 63.61, 77.61 ppm (Fig.

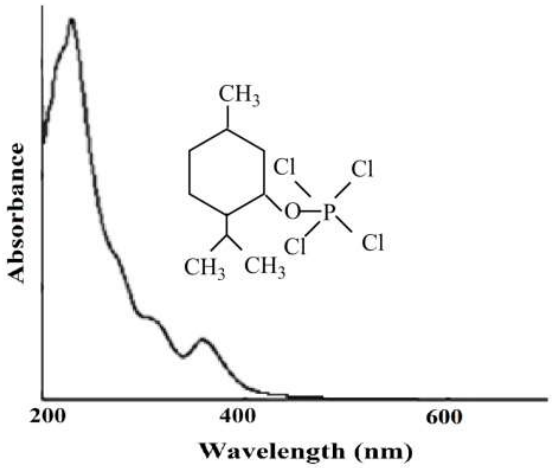

Fig. 3. The UV-Vis spectra of TCMP structure.

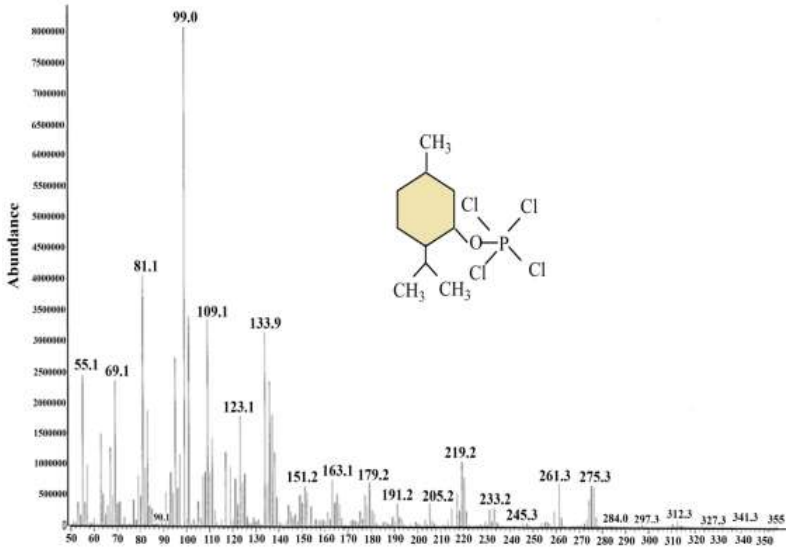

Fig. 4. GC–MS spectra of TCMP structure.

2 (c)). UV-Vis in CH_3CN, λ/cm^{-1}: 280, 320, 380 (Fig.3). In Mass spectra of TCMP a signal at *m/e:* 327 is the basic reason of preparing mentioned organophosphate (Fig. 4). The solubility of the tetrachloromenthoxyphosphor in many solvents is given in the Table 1 at boiling point of 42 °C.

Synthesis of tetrachloromenthoxyphosphor (III)@ TiO_2 (TCMP@TiO_2)

In a regular empirical process, 0.06 g of TiO_2 was distributed in 25 mL of acetic acid (2%) and then 0.06 g of laboratory prepared TCMP was added in 6 mL boiling DIW and poured into the system slowly. The mixed system was vigorously stirred at room temperature for 72 h. Then, the separation of water by evaporation, a gel with white color was prepared. The outcomes can be declare by information of IR (KBr) (cm^{-1}): 3356, 2929, 1456, 1372, 1284, 528, 943, 889, 447, cm^{-1} (Fig.1 (b)).

Decolorization Tests

Dye elimination tests were performed under visible light obtained with a 50 W xenon lamp. Before operating the illumination, the reaction system was stirred for 60 min without the existence of the light to complete the adsorption–desorption equilibrium of the color and the

Table 1. Solubility of the tetrachloromenthoxyphosphor in different solvents.

Solvent	Solubility
DMSO	Solution
Water	Solution
Methanol	Solution
Acetonitrile	Solution
Ethanol	Solution
Chloroform	Solution
Toluene	Solution
Ether	Solution
Hexane	Solution

catalyst. In an empirical experiment, 25 mL of fresh water-based methyl violet mixture with an initial concentration of 60 ppm and 0.02 g of TCMP@TiO_2 prepared catalyst were poured into a 25- mL round-bottom flask. The reaction system was centrifuged at random periods of time. About 3 mL of the solution was used for the spectroscopy evaluation. The sample preparation was applied by a syringe during laboratory works. The methyl violet dye degradation was spectrophotometrically evaluated through calculating the absorbance of the solutions at 410 nm during the photodegradation. The absorption was turned to the concentration operating a standard curve. The dye degradation percentage of methyl violet was calculated using the equation below (Eq. (1)):

$$Decolorization\% = (CM_i - CM_t) / CM_i \times 100 \quad (1)$$

Where, CM_i and CM_t represent the initial and time "t" solution concentrations, respectively.

Optimization of decolorization conditions using RSM

For optimizing the decolorization reaction, DOEs refer to computational methods that are useful tools for researchers to obtain insight into the independent influence of different variables that could affect the research results. In this study, DOEs were done by applying the statistical software Minitab Version 18. To estimate the relationship of a set of processes and response parameters, the DOE computational method was used. Central composite design (CCD) based on response surface methodology (RSM) was applied to develop the situation to obtain the maximal dye removal. Monitored parameters were categorized as temperature (A: 25-40 °C), catalyst dosage (B: 0.005–0.02 g), and C: pH (6–10). All three parameters were tested at three remarked levels (high levels as +1 and lower levels as -1, 0) [18]. Amounts found by 20 experimental data sets suggested by software interceded CCD model in triplicate were contrasted with auspicated once by the model (Table 2). The coefficient of regression was achieved by treating optimized temperature (35 °C), catalyst dosage (0.02 g), and pH (8.0) in present of 1.5 Mm of hydrogen peroxide. Model agreement was confirmed with study of variance pursuing Fisher's statistical data evaluation approach. In this study, DOEs were carried out using statistical software Minitab Version 18.

RESULT AND DISCUSSION

Characterization of TCMP@TiO_2

This research investigated the handling of synthesis a new nanostructure with formula TCMP@TiO_2, through reacting TiO_2 with the tetrachloromenthoxyphosphor (III) in response to the reaction between 2-Isopropyl-5-methylcyclohexanol (menthol) and PCl_5 frequently.

The FT-IR spectra of TMCP and TMCP@TiO_2 are indicated in Fig. 1 where the amount of free OH was determined at 3359 cm^{-1}. The vibrations of aliphatic C-H stretching seen at 2957, 2929, and 2872 cm^{-1}. The absorption at 1456 cm^{-1} was because of asymmetrical bend of CH_3 branch, while a geminal dimethyl doublet was existent at 1386 and 1369 cm^{-1}, the absorption at 1302, 1247, 1209, 1093 cm^{-1} was appointed to C-O stretching. The absorptions at 993, 974, and 932 cm^{-1} which could be assigned to CH_2 rocking vibration were also determined. As shown in Fig 1, under 1300 cm^{-1}, where most of the P-bond vibrations can be detected [19]. Finally, the absorption of P-O observed at 528 cm^{-1} , the 734 and 943 cm^{-1} is showed Ti-O bands vibration. Results for the FTIR of TMCP and TMCP@TiO_2 are listed in Table 3.

The synthesis of nanocatalyst was evaluated

Table 2. Observed values of methyl violet decolorization by TCMP@TiO_2 photocatalyst.

Sr.No	Coded in dependent variable levels			% (Responses)
	Temperatures (A)	Catalyst dosage (B)	pH (C)	Observed value (Experimental)
1	43	0.015	8	56.7
2	35	0.015	8	83.6
3	30	0.02	7	57.2
4	40	0.01	9	59.13
5	35	0.005	8	61.1
6	30	0.02	9	46.3
7	35	0.015	8	83.6
8	35	0.015	8	83.6
9	40	0.02	7	61.2
10	35	0.02	8	83.6
11	35	0.025	8	50.98
12	35	0.015	6.3	72.26
13	35	0.01	8	83.6
14	35	0.015	9.6	57.99
15	35	0.015	8	83.6
16	40	0.02	9	61.61
17	30	0.01	9	55.97
18	40	0.01	7	64.61
19	30	0.01	7	61.95
20	26	0.015	8	56.26

Table 3. FT-IR related to vibration modes of TCMP and TCMP@TiO_2 nanocatalyst.

Vibration mode	$\upsilon_{(cm^{-1})}$	Intensity
TCMP		
v (O-H)	3359	W
v (C-H)	2955	S
v (Ar)	1456	S
v (CH_3)	1369	W
v (C-O)	1302	S
v (P-O)	734	W
v (C-H)	775	W
v (C-Cl)	589	S
v (P-Cl)	484	W
TCMP@TiO2		
v (O-H)	3356	W
v (C-H)	2929	W
v (Ar)	1456	W
v (CH_3)	1372	W
v (C-O)	1284	W
v (Ti-O)	528	S
v (Ti-O)	943	W
v (Ti-Cl)	889	W

through ^{31}P-NMR spectroscopy. The ^{31}P-NMR spectral data of the TCMP molecules are indicated in Fig 2 (a). The solvent applied was $CDCl_3$.The spectral data represents an individual resonance for the phosphorus atom, showing the existence of one type phosphorus in the structure of a central ion whose peak occurs at 5.71 ppm. The chemical shift for ^{31}P is relatively wide. Indeed, the distinct states of phosphorus valence do not follow a certain pattern.

The ^{13}C-NMR and ^{1}H-NMR of TCMP are indicated in Fig 2 (b-c), a raise in the amount of the chemical displacement of the carbons of cyclohexane showed, based on heavy exchange, occurring by distribution of electronic charge all over of these carbon atoms. The peaks of hydrogen atoms in the cyclohexane are recognized empirically from 2.228 to 1.331 ppm. The methyl group hydrogen atom

Table 4. ^{1}H-NMR spectrum of TCMP structure.

Assing.	(ppm)δ	Int.
A	3.7	**-CHO(s)**
B	1.9	**-CH_2(d)**
C	1.6	**-CH_2(d)**
D	1.3	**-$(CH_2)_3$(t)**
E	1.35	**-$(CH_2)_3$(t)**
F	0.9	**-CH_3(d)**

$C_{10}H_{20}O$: F E D C B A
CH_3-$(CH_2)_3$-$(CH_2)_3$-CH_2-CH_2CHO

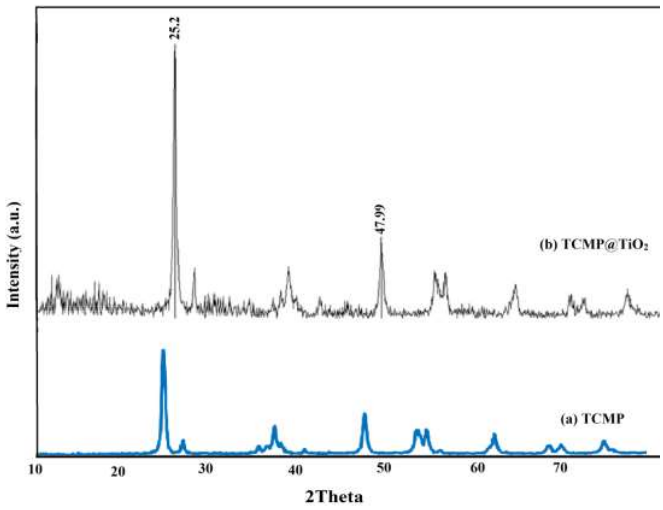

Fig. 5. XRD pattern of (a) TCMP, (b) TCMP@TiO_2.

determined at 0.9 ppm is the minimum chemical displacement in all hydrogen atoms. Apparently, it is because its electrostatic interaction with other atoms is minor. The chemical displacement in CHO ^{1}H-NMR produced a lone signal in 3.7 ppm CH_2 next to the CHO functional group raises in 1.9 ppm and the next one comes in 1.6 ppm (see Table 4).

The structure of the TiO_2 binding with TCMP was studied applying UV-Vis spectroscopy. Because of the absence of chromophore (colored) agents, no transition was seen in the visible region that is a confirmation for the colorlessness of the molecules. In Fig. 3, the observed transitions in the UV-Vis spectrum are seen in the part below 400 nm, showing the $n\rightarrow\pi^*$ transitions.

In the present study, the GC–MS spectra of TCMP are shown in Fig. 4. Commonly, the molecular ion peak excitement of a first or second type alcohol is very negligible in the mass spectrum and indicates a very weakened molecular ion peak in the TCMP complex MASS spectrum of the Fig. 4 peak interrelated to M/e =327 molecular mass. It is indicated that there is a credible sense for the preparing of this compound, seeing that isotopes of chlorine (^{35}Cl, ^{37}Cl) and carbon (^{13}C, ^{12}C) of many peaks can be recognized.

The crystalline structure of the catalyst was analyzed applying the XRD method to determine the composition of TCMP@TiO_2 photocatalyst. The patterns were collected within the scanning range of $10° \leq 2\theta \leq 80°$ as indicated in Fig. 5. Based on the usage of titanium dioxide in this experiment contains the anatase and a bit rutile phase the producing spectrum has peaks composed of both phases. Forceful diffraction peaks at 25°and 48° showing TiO_2 anatase phase and diffraction peaks at 27° and 55° representing TiO_2 in rutile phase (Fig.5 (a)). By comparing the X-ray diffraction patterns of TCMP@TiO_2 hybrid nanocatalyst (Fig.5 (b)) with that of pure TiO_2, it could be found that the sharp peaks at 24.95°, 37.90°, 48.0°, 55°, 62.7°, and 75.0° are due (101), (004), (200), (105), (204), and (215) crystal planes of anatase titanium dioxide [20–23].

Interestingly, a thorough examination of the X-ray diffraction patterns revealed a shift

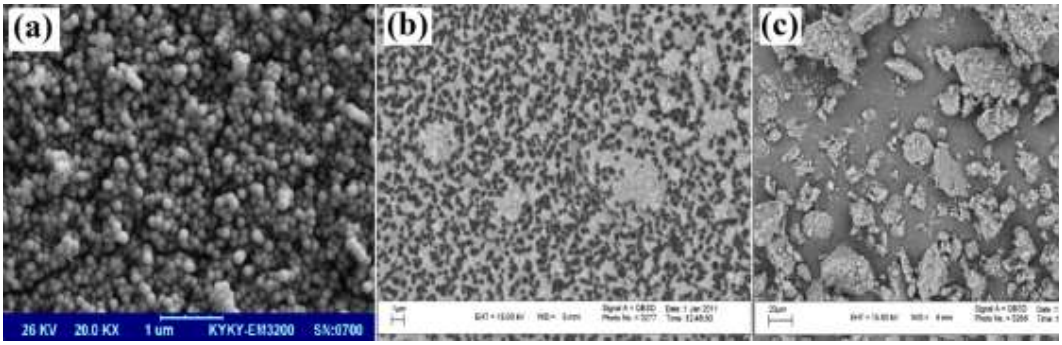

Fig. 6. SEM images of (a) TiO2, (b) TCMP, and (c) TCMP@TiO_2.

in the peak positions of the TCMP@TiO_2 hybrid nanocatalyst toward a higher angle compared to bulk titanium dioxide. Further, the doping of tetrachloromenthoxyphosphor (III) in the titanium dioxide generates residual stress in the matrix, which leads to a shift of the characteristic diffraction angle of titanium dioxide [24-25]. These slight shifts in the modified nanocatalyst TCMP@TiO_2 proved the intermolecular electronic interactions between titanium dioxide and phosphorus. In addition, the X-ray diffraction patterns of hybrids TCMP@TiO_2 are in good agreement with FT-IR results. The nanocrystallite size of the hybrid nanocatalyst is estimated by the Debye–Scherrer equation (Eq. (2)).

$$D \text{ ¼ } K \lambda = \beta \cos \theta \quad (4)$$

Where, D is mean size of crystallites, K is equal to 0.89, λ denotes the X-ray wavelength for Cu Kα radiation (1.5406 Å), β is the Full Width at Half Maximum (FWHM), and θ shows the half of the diffraction angle [26]. According to this equation, the average size of the TCMP@TiO_2 is estimated to be about 10.26 nm.

As further evidence, the surface morphology of hybrid nanocatalyst was studied using SEM technique. The SEM images of the composite are displayed in Fig. 6. The prepared TCMP@ TiO_2 nanocomposite showed the sphere-like morphology (Fig 6(a)) with a mean particle size of ∼11 nm for the prepared photocatalyst. The excellent catalytic efficiency of the new hybrid catalyst might be explained by surface morphology, which provides a good catalytic structure for scavenging of dye molecules (Fig 6(b, c)).

Optimization of the decolorization process by RSM

TCMP@TiO_2 was exposed to various temperature, catalyst dosage, and pH for maximal color removal. Likewise, H_2O_2 operate as depot electron accepter in the chemical reaction process which was catalyzed by oxidants [27]. The amounts of H_2O_2 has direct effect on dye removal interfered by incapacitated peroxidases. So, in this work we perform all of experiments in present of 1.5 mM of hydrogen peroxide. Dye removing optimization of MV applying TCMP@TiO_2 utilizing response surface methodology seeing optimal situation (temperature 35 °C, catalyst dosage 0.02 g, and pH 8.0 in present of 1.5 Mm of hydrogen peroxide) indicated statistically proper model with R-square amount of 0.9275. This amount of R^2 value, that is for decolorization process of MV, indicating with appropriate correlation of anticipated and recognized reflections. The description of curve plots with their and structure as circular and elliptical explain the interaction of parameters treated for research. Elliptical plots explained important interaction, because, circular plots represent the same interactions [28-29]. 3D plot represented a rise in the dye removal along with a rise in optimal effecting variables; it again demonstrated that, every variable has unique response on useful dye elimination. These plots indicated a rising in the dye elimination along with a rising in optimal effecting variables. Every variable had unique effect on the useful color elimination. The response for the quadratic polynomials is as follows:

$$Y = \beta_0 + \sum \beta_i X_i + \sum \beta_{ij} X_i^2 + \sum \beta_{ij} X_i X_i \quad (3)$$

where (Y) is the efficiency of decolorization, (X_i) is the independent factor level, (i) is the independent factor level, (β_0) is the process effect on the constant-coefficient, (β_i) is the linear coefficient, (β_{ii}) is the quadratic effect of (X_i), and

Table 5. Analysis of variance for the response surface quadratic model.

Source	DF	Adj SS	Adj MS	F-Value	P-Value
Model	9	2843.55	315.95	14.22	0.000
Linear	3	328.54	109.51	4.93	0.024
A	1	121.01	121.01	5.45	0.042
B	1	81.07	81.07	3.65	0.085
C	1	123.95	123.95	5.58	0.040
Square	3	2523.62	841.21	37.87	0.000
A*A	1	1503.91	1503.91	67.71	0.000
B*B	1	1213.79	1213.79	54.65	0.000
C*C	1	835.45	835.45	37.61	0.000
2-Way Interaction	3	40.30	13.43	0.60	0.627
A*B	1	22.75	22.75	1.02	0.335
A*C	1	17.43	17.43	0.78	0.396
B*C	1	0.12	0.12	0.01	0.943
Error	10	222.12	22.21		
Lack-of-Fit	7	222.12	31.73	*	*
Pure Error	3	0.00	0.00		
Total	19	3065.67			

SS Sum of squares, DF degree of freedom, MS mean of squares.

(β_{ij}) is the effect of interaction between (X_i) and (X_j) on the decolorization reaction. By applying multiple regression analysis, the second-order polynomial equation (in coded units) that could relate decolorization to the factor evaluated was achieved as Eq. (4):

$$Y = -848 + 25.54A + 5752B + 114.3C - 0.4102A^2 - 290059B^2 - 8.05C^2 + 67.5AB + 0.295AC + 24BC \quad (4)$$

where (Y) is decolorization efficiency, (A) is the coded value of temperatures range of the decolorization media, (B) is the coded value of different catalyst dosage, and (C) is the coded value of different pH. As decolorization results, the observed and predicted values presented that the experimental models were the same as the actual data with R-square of 0.9275. As obtained in this research, when the R-square is closer to one the experimental models fit better the actual data, while the correlation of the dependent parameters in the model in presenting the behavior of differentiation cannot be identified by a smaller value of R^2. The analysis of variance (ANOVA) results for the response surface quadratic model are listed in Table 5. The F-value of the model was 14.22 and the p-value for the model was <0.05, which point that it is eligible and desirable as it indicates that the terms in the model have a significant effect on the response. So, with a p>0.05, it can be confirmed that the model terms are not effective and important. The p-value less than 0.0001 prove that there is only a 0.01% chance that an F-value model could occur due to noise in the experiment media. In this work, A, B, C, A^2, B^2, C^2, AB, AC, and BC were effective model terms. The chosen values for the level merger of the three effective parameters of temperature dye removal process, amount of catalyst, and pH are presented in (Fig 7) which shows the decolorization performance. Fig. 7 (a) shows the function of the dye removal efficiency with changes in temperature and catalyst amount. These two parameters had a positive effect on dye removal. The dye removal performance increased with increases in catalyst dosage and temperature. As shown in Fig. 7 (a), the differentiation of decolorization efficiency as identified by temperature and catalyst dosage showed that by increasing process temperature, efficiency of decolorization increased to a certain rate and further increase in the process temperature to the 40 °C did not show any significant effects on the

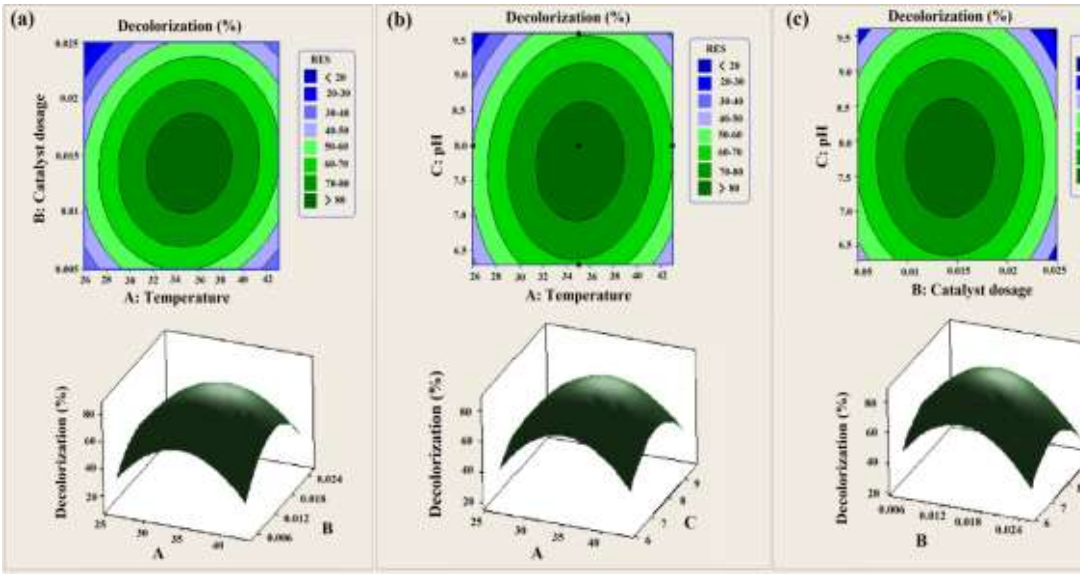

Fig. 7. Contour plot and 3D surface showing dye decolorization extent as a function of (a) temperature and catalyst dosage (Actual factor C: pH = 8), (b) temperature and pH (Actual factor B: catalyst dosage = 0.02 g.), and (c) catalyst dosage and pH (Actual factor A: temperature = 35 °C) in the presence of 1.5 mM of hydrogen peroxide.

dye removal and degradation reaction, potentially due to enhanced decomposition of H_2O_2 over TCMP@TiO_2 catalyst at higher temperatures (Fig. 7 (b)). The optimized degradation performance was obtained with a temperature at 35 °C and 0.02 g of catalyst dosage. The plots for the effects of interaction due to catalyst amount and pH on yield of decolorization process are presented in Fig. 7 (c). Efficiency of degradation increased as dosage of catalyst increased to its optimized rate (0.02 g) and pH increased to its optimal rate (8.0). In each contour plot, the other parameter was kept at a constant rate. Accordingly, increases in the three reaction variables to optimized values resulted in an increase in decolorization of methyl violet by the TCMP@TiO_2 heterogeneous catalyst. As presented in equation 4, this is as a result of the positive quadratic model. It is significant that the laboratorial value must consider the performing effect of these remarkable factors at the stipulated rate to maximize the removal of methyl violet by the TCMP@TiO_2 nanocomposite. Moreover, in order to evaluate the achieved data from the CCD, five validation tests determined in the optimal process were estimated by applying RSM. For the optimized reaction, the software proposed five ways based on the order of adaptability, one of which was chosen for further studies to prove the validity of the statistical test with the laboratory data. The optimal decolorization conditions were temperature = 35 °C, catalyst dosage = 0.02 g, and pH = 8.0 in the present of 1.5 mM of H_2O_2. The mean degradation rate was 83.6% from a concentration of 60 ppm MV arouse solution. The data proved the predictability of the model for the decolorization under laboratory conditions.

Proposed mechanism for decolorization

As reported studies [29-30], the production of hydroxyl group radicals and its relation with photoactivity can be explained by the reaction mechanism below:

$$TiO_2 + hv \rightarrow e^- + h^+ + \text{heat}$$

The produced holes in TiO_2 formation are applied for producing hydroxyl group radicals and direct oxidation of MV or they can be connected with the electron from a donor species [31].

$$Ti^{IV} - OH^- + h^+ \rightarrow Ti^{IV}\text{-}OH^{\bullet}$$

$$Ti^{IV} - H_2O + h^+ \rightarrow Ti^{IV}\text{-}OH^{\bullet} + H^+$$

$$MV_{ads} + h^+ \rightarrow MV_{ads}^{+}$$

The existence of hydrogen peroxide in the system can encourage the production of more radicals:

$$Ti^{IV}\text{-}OH^{\bullet} + H_2O_2 \rightarrow Ti^{IV} + HO^{\bullet}{}_2$$

$H_2O_2 + {}^{\bullet}OH \rightarrow H_2O + HO^{\bullet}{}_2$

HO_2+ MV → Oxidation of MV

CONCLUSION

A novel TCMP@TiO_2 photocatalyst was designed and synthesized successfully by promoting tetrachloromenthoxyphosphor (III) on TiO_2 for elimination of MV from water media. The optimal dye degradation condition included: temperature = 35 °C, catalyst dosage = 0.02 g, and pH = 8.0. The mean dye removal achieved was 83.6% from an amount of 60 ppm methyl violet aqueous solution. Excellent elimination of methyl violet utilizing the TCMP@TiO_2 suggests its high dye removal potential for real industrial applications in the degeneration of synthetic dye effluents.

DECLARATION OF COMPETING INTEREST

The authors declare that they have no known competing financial interests or personal relationships that could have appeared to influence the work reported in this paper.

REFERENCES

1. Robinson T., McMullan G., Marchant R., Nigam P., (2001), Remediation of dyes in textile effluent: a critical review on current treatment technologies with a proposed alternative. *Bioresour. Technol*. 77: 247-255.
2. Hammami S., Bellakhal N., Oturan N., Oturan M. A., Dachraoui M., (2008), Degradation of Acid Orange 7 by electrochemically generated OH radicals in acidic aqueous medium using a boron-doped diamond or platinum anode: A mechanistic study. *Chemosphere*. 73: 678-684.
3. Melgoza D., Hernandez-Ramirez A., Peralta-Hernandez J. M., (2009), Comparative efficiencies of the decolourisation of Methylene Blue using Fenton's and photo-Fenton's reactions. *Photochem. Photobiol. Sci.* 8: 596-599.
4. Pare B., Jonnalagadda S. B., Tomar H., Singh P., Bhagwat V. W., (2008), ZnO assisted photocatalytic degradation of acridine orange in aqueous solution using visible irradiation. *Desalination*. 232: 80-90.
5. Yassıtepe E., Yatmaz H. C., Öztürk C., Öztürk K., Duran C., (2008), Photocatalytic efficiency of ZnO plates in degradation of azo dye solutions. *J. Photochem. Photobiol*. 198: 1-6.
6. Kong J. Z., Li A. D., Li X. Y., Zhai H. F., Zhang W. Q., Gong Y. P., Wu D., (2010), Photo-degradation of methylene blue using Ta-doped ZnO nanoparticle. *J. Solid State Chem.* 183: 1359-1364.
7. Cozzoli P. D., Kornowski A., Weller H., (2003), Low-temperature synthesis of soluble and processable organic-capped anatase TiO2 nanorods. *J. Am. Chem. Soc.* 125: 14539-14548.
8. Jun Y. W., Jung Y. Y., Cheon J., (2002), Architectural control of magnetic semiconductor nanocrystals. *J. Am. Chem. Soc.* 124: 615-619.
9. Rao, A. R., Dutta, V., (2007), Low-temperature synthesis of TiO_2 nanoparticles and preparation of TiO_2 thin films by spray deposition. *Sol. Energy Mater Sol. Cells. 91*: 1075-1080.
10. Xue X. D., Fu J. F., Zhu W. F., Guo X. C., (2008), Separation of ultrafine TiO_2 from aqueous suspension and its reuse using cross-flow ultrafiltration (CFU). *Desalination*. 225: 29-40.
11. Fatimah I., Said A., Hasanah U. A., (2015), Preparation of TiO_2-SiO_2 using rice husk ash as silica source and the kinetics study as photocatalyst in methyl violet decolorization. *Bull. Chem. React. Eng. Catal.* 10: 43-49.
12. Liu G., Niu P., Yin L., Cheng H. M., (2012), α-Sulfur crystals as a visible-light-active photocatalyst. *J. Am. Chem. Soc.* 134: 9070-9073.
13. Liu G., Niu P., Cheng H. M., (2013), Visible-light-active elemental photocatalysts. *Chem. Phys. Chem*. 14: 885-892.
14. Arzehgar Z., Hosna A., (2019), A convenient one-pot method for the synthesis of symmetrical dialkyl trithiocarbonates using NH_4OAc under mild neutral conditions. *J. Chin. Chem. Soc*. 66: 303-306.
15. Soleiman-Beigi M., Arzehgar Z., (2013), A review study on chemical properties and food indexes of mastic Oil compared with Olive, sunflower and canola oils. The Ilamian traditional uses of mastic. *J. Ilam Uni. Med. Sci*. 21: 1-13.
16. Sadegh-Malvajerd S., Arzehgar Z., Nikpour F., (2013), Regio-and Chemoselective Synthesis of 5-Aroyl-NH-1, 3-oxazolidine-2-thiones. *Z. Naturforsch B. J. Chem. Sci*. 68: 182-186.
17. Yew S. P., Tang H. Y., Sudesh K., (2006), Photocatalytic activity and biodegradation of polyhydroxybutyrate films containing titanium dioxide. *Polym. Degrad. Stab.* 91: 1800-1807.
18. Bhalkar B. N., Bedekar P. A., Patil S. M., Patil S. A., Govindwar S. P., (2015), Production of camptothecine using whey by an endophytic fungus: standardization using response surface methodology. *RSC advances*. 5: 62828-62835.
19. Ansari S. A., Cho M. H., (2017), Growth of three-dimensional flower-like SnS_2 on gC_3N_4 sheets as an efficient visible-light photocatalyst, photoelectrode, and electrochemical supercapacitance material. *Sustain. Energy Fuels*. 1: 510-519.
20. Khan M. M., Ansari S. A., Pradhan D., Ansari M. O., Lee J., Cho M. H., (2014), Band gap engineered TiO_2 nanoparticles for visible light induced photoelectrochemical and photocatalytic studies. *J. Mater. Chem. A*. 2: 637-644.
21. Ansari S. A., Khan M. M., Ansari M. O., Cho M. H., (2016), Nitrogen-doped titanium dioxide (N-doped TiO_2) for visible light photocatalysis. *New J. Chem*. 40: 3000-3009.
22. Ansari S. A., Khan M. M., Ansari M. O., Cho M. H., (2015), Gold nanoparticles-sensitized wide and narrow band gap TiO_2 for visible light applications: A comparative study. *New J. Chem*. 39: 4708-4715.
23. Li W. J., Chou S. L., Wang J. Z., Liu H. K., Dou S. X., (2013), Simply mixed commercial red phosphorus and carbon nanotube composite with exceptionally reversible sodium-ion storage. *Nano Lett.* 13: 5480-5484.
24. Kang Q., Cao J., Zhang Y., Liu L., Xu H., Ye J., (2013), Reduced TiO_2 nanotube arrays for photoelectrochemical water splitting. *J. Mater. Chem. A*. 1: 5766-5774.
25. Wang S., Zhao L., Bai L., Yan J., Jiang Q., Lian J., (2014),

Enhancing photocatalytic activity of disorder-engineered C/TiO_2 and TiO_2 nanoparticles. *J. Mater. Chem. A.* 2: 7439-7445.

26. Khanmohammadi Khorrami M. R., Shokri Aghbolagh Z., (2020), Synthesis and non-parametric evaluation studies on high performance of catalytic oxidation-extraction desulfurization of gasoline using the novel TBAPW_{11}Zn@TiO_2@PAni nanocomposite. *Appl. Organomet. Chem.* 34: e5299.
27. Pearse I. S., Heath K. D., Cheeseman J. M., (2005), Biochemical and ecological characterization of two peroxidase isoenzymes from the mangrove, Rhizophora mangle. *Plant Cell Environ.* 28: 612-622.
28. Aghbolagh Z. S., Khorrami M. R. K., Rahmatyan M. S., (2020), Fabrication of $(C_4H_9)_4$NPZnW_{11}-TiO_2/PANI as an efficient nanocatalyst for dye degradation. *Chem. Select*. 5: 9424-9430.
29. Zhang H., Lv X., Li Y., Wang Y., Li J., (2010), P25-graphene composite as a high performance photocatalyst. *ACS Nano*. 4: 380-386.
30. Choi H., Al-Abed S. R., Dionysiou D. D., Stathatos E., Lianos P., (2010), TiO_2-based advanced oxidation nanotechnologies for water purification and reuse. *Sustain Sci. Eng.* 2: 229-254.
31. Herrmann J. M., Duchamp C., Karkmaz M., Hoai B. T., Lachheb H., Puzenat E., Guillard C., (2007), Environmental green chemistry as defined by photocatalysis. *J. Hazard. Mater.* 146: 624-629.